ACADEMIA ROMÂNĂ
Revue Roumaine de Chimie
http://web.icf.ro/rrch/

Rev. Roum. Chim.,
2016, *61*(11-12), 857-862

EFFECT OF THE SOLVENT ON THE MORPHOLOGY AND THE SIZE OF ZnO NANOPARTICLES SYNTHESIZED IN POLYOL MEDIUM

Bilel CHOUCHENE,[a] Karima HORCHANI-NAIFER[b] and Tahar BEN CHAABANE[a,*]

[a] Unité de Recherche UR11ES30, Université de Carthage, Faculté des Sciences de Bizerte, 7021 Jarzouna,Tunisie
[b] Laboratoire de Physico-Chimie des Matériaux Minéraux et leurs Applications, Centre National des Recherches en Sciences des Matériaux, Technopole de Borj Cedria, BP 73, 8027 Soliman, Tunisie

Received February 12, 2016

Zinc oxide (ZnO) nanocrystals were successfully synthesized using a simple polyol process using two solvents: ethylene glycol (EG) and diethylene glycol (DEG). The effects of the hydrolysis ratio and the polyol structure on the shape and the size of the ZnO particles were mainly examined. It was found that the solvent structure and the polarity of the medium played a great role in determining the nanoparticles morphology. Quasi-spherical particles were obtained in EG for all values of hydrolysis ratio h ($2 \leq h \leq 30$), nevertheless nanorods were formed in DEG when the hydrolysis ratio (h) is lower ($h < 10$). Possible growth mechanism of the prepared ZnO nanocrystals is also proposed and discussed.

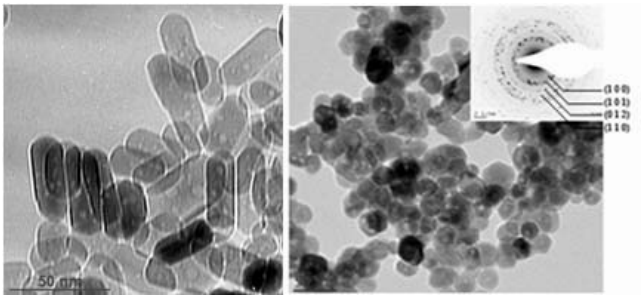

INTRODUCTION

Zinc oxide ZnO has attracted much interest because of its promising applications in nanoscience and nanotechnology such as room-temperature UV lasers, gaz sensors, solar cells, photocatalysts....[1-5] The syntheses of ZnO nanoparticles in liquid medium using water or organic solvent such as hydrothermal or solvothermal process, sol-gel technique, polyol process… offer advantages of low-temperature processing and potential inexpensive manufacturing of zinc oxide material.[6-9]

The polyol process has already proved its efficiency to lead to nanoscale particles of different kinds: metals, oxides or hydroxides elaborated with good cristallinity and narrow size distribution.[10-13] Lee *et al.*[14] have prepared ZnO nanocrystals in diethylene glycol DEG at 180° and the particles morphology was controlled by adjusting the hydrolysis ratio h in the reduced range: $4 \leq h \leq 8$. Dakhlaoui *et al.*[15] have synthesized ZnO particles in polyol medium and have found that the alkaline ratio value plays a great role in controlling the shape and the size of the particles. In our study, the effect of a large range of the hydrolysis ratio h ($2 \leq h \leq 30$) was mainly investigated using two solvents: DEG and EG. The evolution of the particles morphology was strongly dependent not only on the hydrolysis ratio but also on the nature of the polyol.

SYNTHESIS AND CHARACTERIZATION

Zinc acetate dihydrate (0.5 M), sodium hydroxide (1M) and appropriate amount of distilled water were dissolved in 50 ml of

* Corresponding author: Taharbch@yahoo.com

diethylene glycol (DEG) or ethylene glycol (EG) and then heated at a constant rate of 6 °C/min to reach a fixed reaction temperature T_R for 4 hours under continuous mechanical agitation. After cooling to room temperature, each sample was centrifuged and the obtained powder was washed several times with ethanol and acetone, and then dried in air at 60°C.

X-ray powder diffraction (XRD) patterns were recorded on a Bruker D8 Advance apparatus in the 2θ range 10-80° with Cu (Kα radiation (1.5406 Å). The average crystallite sizes were calculated from the width of the XRD peaks using the Scherrer formula.[16] Transmission electron microscopy (TEM) images were taken using a Philips CM20 TEM operating at 200 kV. The UV-visible absorption spectra of ZnO nanoparticles dispersed in ethanol were performed on a Perkin Elmer lambda 11 spectrometer. Fourier transform infrared (FT-IR) spectra were recorded on a Thermo Scientific Nicolet IR 200 spectrophotometer in the range of 400-4000 cm^{-1}.

RESULTS AND DISCUSSION

The hydrolysis ratio h ($h = n_{water} / n_{Zinc}$) and the polyol structure were the main synthesis parameters used to control the size and the shape of the ZnO particles.

The hydrolysis parameter h was varied between 2 and 30, the alkaline ratio b ($b = n_{sodium\ hydroxide} / n_{Zinc}$) was fixed to 2 for all samples. It is worth to note that the reaction temperature T_R corresponded to the boiling temperature of the mixture and depended on the hydrolysis ratio h: T_R decreased when the ratio h increased (Table 1).

1. XRD study

All the diffraction peaks of the XRD patterns of all samples are matching well with ZnO wurtzite structure reported in JCPDS card (N° 36-1451, a = 0.3253 nm, c = 0.5210 nm). Typical XRD patterns are given in Fig. 1 and reveal well-crystallized and pure ZnO nanocrystals.

Table 1

Main results obtained as a function of various synthesis parameters*

Sample	Hydrolysis ratio (h)	Temperature T_R (°C)	Polyol solvent	Powder morphology
D2	2	180	DEG	Mostly nanorods
E2	2	180	EG	Quasi-spherical
D5	5	180	DEG	Nanorods
E5	5	180	EG	Spherical
D10	10	170	DEG	Elliptical
D20	20	140	DEG	Elliptical
E20	20	140	EG	Spherical
D30	30	130	DEG	Quasi-spherical
E30	30	130	EG	Spherical

* The alkaline ratio was fixed to b = 2.

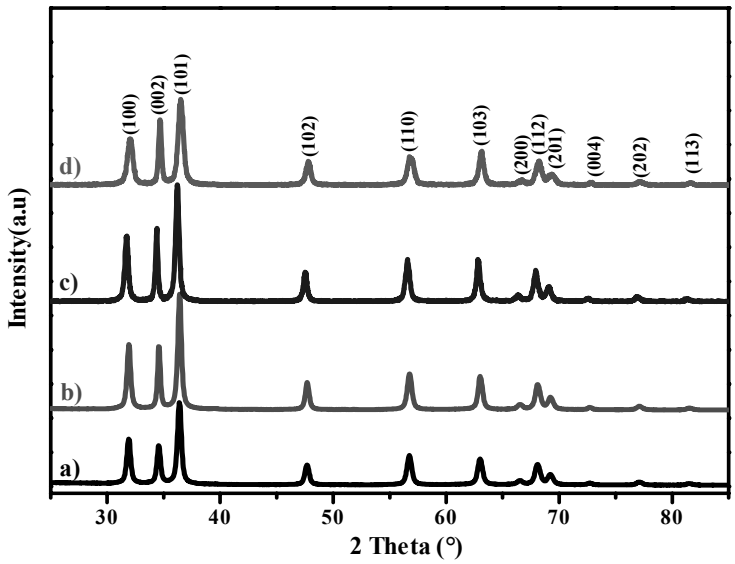

Fig. 1 – XRD diffraction patterns of synthesized ZnO particles, a) E30; b) E20; c) D10; d) D5.

Comparison of all the diffraction patterns revealed a visible variation of the peaks intensity for (100), (002) and (101) (hkl) planes. The intensity ratios $R = I_{(002)}/I_{(100)}$, given in Table 2, depend on the particles morphology. The R values which are higher than the unity indicate preferential growth of the particles along the c-direction.

The biggest intensity ratio (1.30) was noticed for D5. For all the nanocrystals synthesized in EG, the intensity ratios R are lower than the unity (Table 2) and the corresponding particles are quasi-spherical. The calculated crystallite sizes from the full width at half maximum (FWHM) of (1 0 0) and (1 0 1) peaks are almost similar, whereas those obtained from (0 0 2) one exhibit a slight increase, mainly noticed for D5, which further confirms the orientation growth of the particles along the c axis corresponding to the [0 0 1] direction.

2. FT-IR spectroscopy analysis

The infra-red spectra of the as-prepared particles presented similar characteristics for all samples. IR spectra of D5 and E5 prepared in DEG and EG respectively, are given in Fig. 2.

The broad band centred at 3414 cm^{-1} is attributed to O-H stretching vibration arising from different hydroxyl groups of the adsorbed polyol, residual ethanol and water. Bands between 3000 and 2850 cm^{-1} are due to C-H stretching vibration of the DEG or EG. The peaks located in 2240-2000 cm^{-1} region are assigned to the bending mode of the OH groups of water and solvent.[15] The two bands observed at 1590 and 1426 cm^{-1} are due to the asymmetrical and symmetrical stretching of the zinc carboxylate (COO^-) respectively.[17] The bands appearing in 1130-1060 cm^{-1} region are attributed to the stretching mode of C-OH bond of the solvent; the corresponding bending vibration is located around 909 cm^{-1}. The intense peak located at 438 cm^{-1} with a shoulder at ca 500 cm^{-1} is characteristic of zinc oxide and it is due to Zn-O vibration.[18, 19] Hence, from this analysis, it is concluded that polyol molecules (DEG or EG) and water were actually adsorbed on the surface of the ZnO particles.

3. TEM analysis

TEM micrographs of the samples E5, E30 and D5 are shown in Fig. 3a-c. The diffraction rings of the selected area electron diffraction (SAED) pattern (inset of Figs. 3b and 3c) proved the polycrystalline character of the samples and permitted to identify the planes (1 0 0), (1 0 1), (0 1 2) and (1 1 0) of the wurtzite-type ZnO structure. One can notice a clear difference between the TEM images of D5 and E5 (Figs. 3a and 3b) prepared in different solvents but under the same experimental conditions. Nanorods with an average length of 44 nm and an average diameter of 16 nm were observed for D5 whereas spherical particles with an average size of 14.5 nm were obtained for E5. The same spherical morphology with a large diameter of 29 nm was obtained in EG when the hydration ratio is higher (E30, Fig. 3c). Note that ethylene glycol with dielectric constant of 37.7 is more polar than DEG with dielectric constant of 31.8.[20] It is worth noting that the polyol acts as surfactant ligand and its presence on the particles surfaces was clearly supported by the FT-IR analysis. Comparing to DEG, ethylene glycol exhibiting shorter chain length and relatively higher polarity, would be better adsorbed on polar as well as on non-polar surfaces of the nanocrystals with a quasi-homogeneous manner. Consequently, the particles growth was carried out in all directions with comparables velocities leading to spherical particles. Note that such isotropic morphology was actually obtained in EG regardless of the hydrolysis ratio.

In the case of DEG, the molecules of the solvent could be differently adsorbed on the surfaces, the polar (0 0 1) and (0 0 $\bar{1}$) planes would be less covered by the molecules of the DEG because of its lower polarity. As a result, the particle growth may be preferentially improved along the polar c axis leading to nanorods (D5) instead of nanospheres (E5). Increasing the hydration ratio h from 2 to 30 results in a visible change of the particles morphology that evolved in DEG from rod shape to quasi-spherical one (Fig. 4a and 4b). The particle growth is obviously affected by the hydration ratio; therefore it is mainly governed by the process of hydrolysis and condensation reactions of the zinc precursor as previously proposed by Lee et al. [14]. At the hydrolysis ratio of 2, mostly nanorods were obtained with a shorter average length of 35 nm and a little aspect ratio of 2.2. However, when the hydration ratio was elevated to 5, sufficient water was present to improve the hydrolysis of the Zinc acetate on the (0 0 1) and (0 0 $\bar{1}$) polar planes.

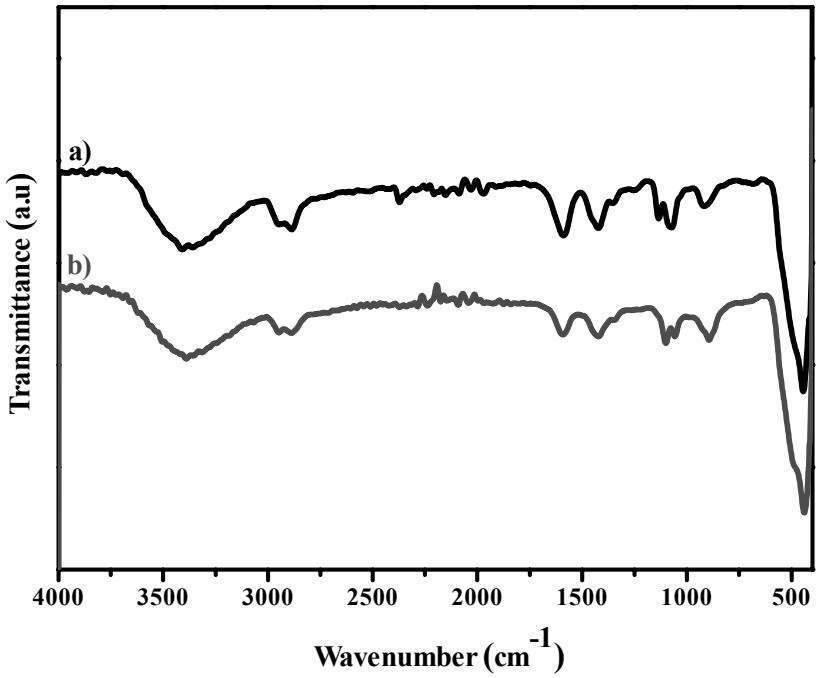

Fig. 2 – FT-IR spectra of ZnO particles: a) D5; b) E5.

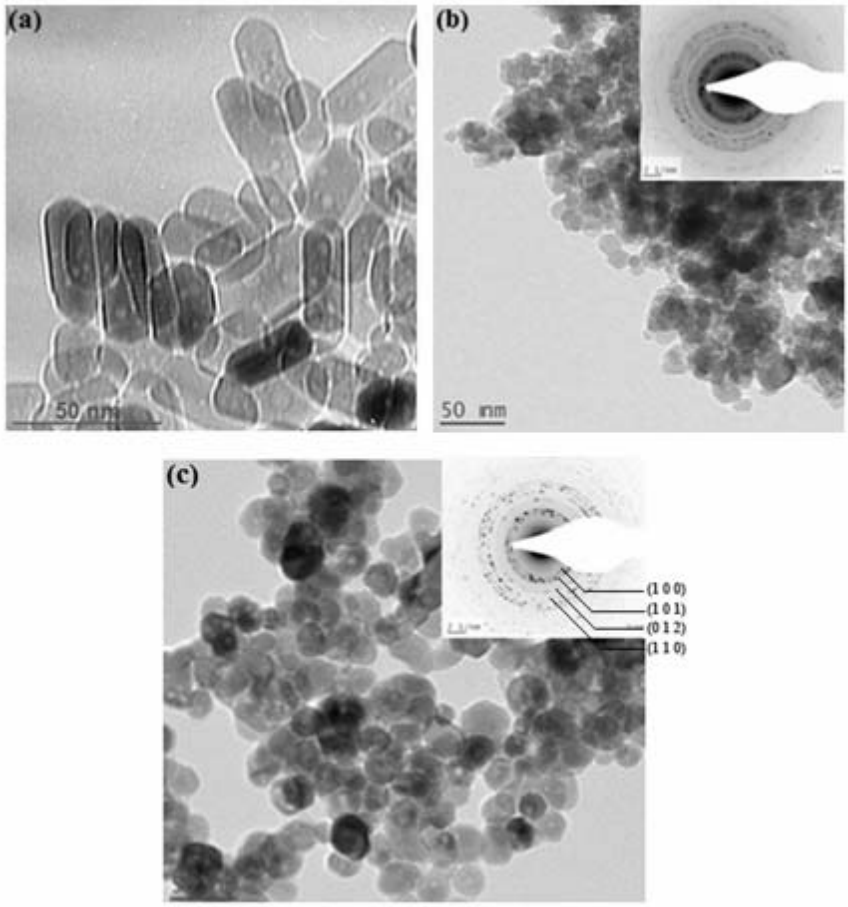

Fig. 3 – TEM images of the as-prepared ZnO particles: a) D5; b) E5; c) E30.

As a result, the nanorods were elongated to reach an average length of 45 nm and an aspect ratio of 3 (Table 2). Further increasing the water amount to h = 10, 20 or 30, the hydrolysis reaction can occur on the surface of other planes and the ZnO can grow in different directions leading to quasi-spherical particles.

4. UV-visible spectroscopy

Room-temperature UV-Visible absorption spectra are given in Fig. 5. In order to determine a precise measure of the absorption edges, we use the method of the point of inflection, obtained from the minimum in the first derivative curve of the absorption spectrum [21,22] (Table 2). The values of Eg are ranging from 3.31 to 3.33 eV and are in good agreement with the band gap of the bulk ZnO solid (3.37 eV). As expected, no size confinement effect was observed because the as-prepared particles are much larger than the ZnO exciton Bohr radius of 2.34 nm.[23]

Table 2

Structural Characteristics, average sizes and gap energy of the as-prepared ZnO particles

Sample	Intensity ratio $I_{(002)}/I_{(100)}$	Crystallites sizes (nm) Calculated from the peaks*			Observed overage dimensions (nm) of the particles			Gap E_g (eV)
		(100)	(002)	(101)	Length	Diameter	A.R**	
D2	1.05	19	28	18.6	35	16	2.2	3.32
E2	0.84	14	14.6	13		12		
D5	1.30	19	39.6	19.4	44	16	2.8	3.33
E5	0.91	15	17.7	15		14.5		3.33
D10	1.03	25.8	38.3	25.5		20-28		
D20	1.08	27	33	26.6		25-35		
E20	0.98	24.7	34.7	25.5		28		
D30	0.93	35	40.4	34		38		3.31
E30	0.81	23.5	27	23		29		3.32

* Using the Sherrer formula.[16]; **A.R: Aspect Ratio.

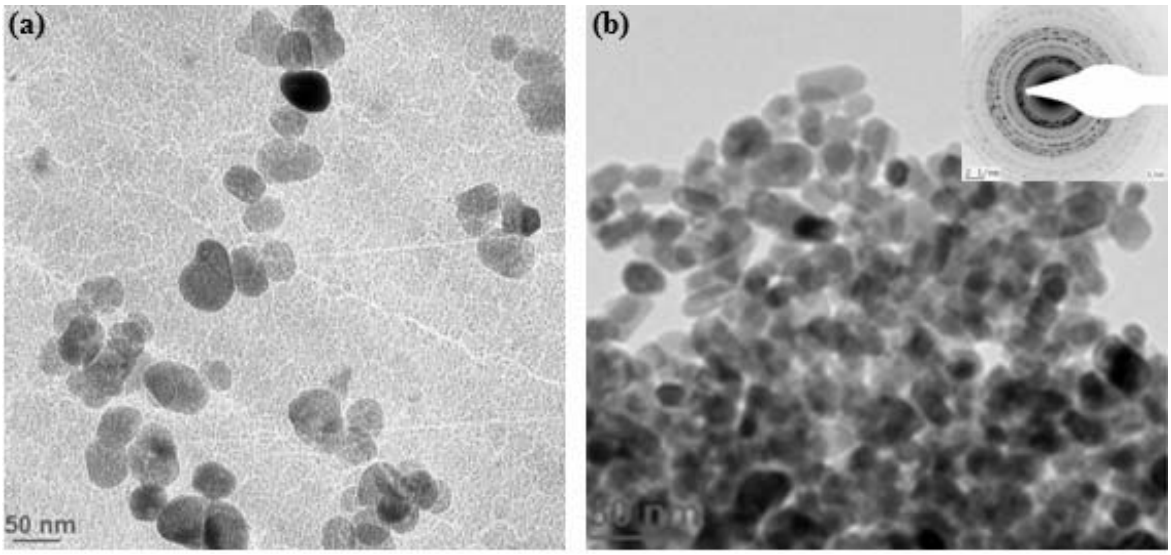

Fig. 4 – TEM images of the sample: a) D30 (quasi-spherical); b) D2 (mostly nanorods).

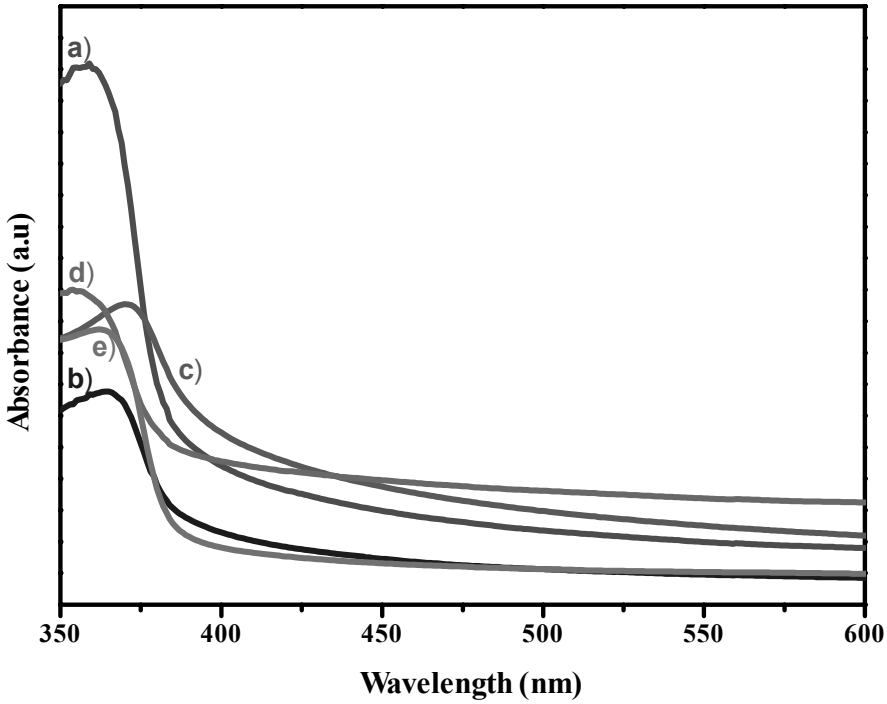

Fig. 5 – UV–Vis absorption spectra of ZnO particles: a) E30, b) D30, c) D2, d) E5, e) D5.

CONCLUSION

In summary, ZnO nanoparticles with wurtzite crystal structure and good cristallinity have been synthesized using a simple polyol process. The size and the morphology of the particles were mainly dependent on the polyol structure, its polarity and the water amount. Our results clearly showed that DEG and EG have different behavior in controlling the particles morphology. The EG solvent was favourable to obtain spherical nanoparticles whereas nanorods can be formed in DEG when the hydrolysis ratios are low (h=2–5).

Acknowledgements: The authors are very thankful to Professor Raphael Schneider (LRGP, University of Nancy, France) for his help in acquiring TEM analysis.

REFERENCES

1. T. Krishnakumar, R. Jayaprakash, N. Pinna, V.N. Singh, B.R. Mehta and A.R. Phani, *Mater. Lett.*, **2008,** *63,* 242-245.
2. Z. Deng, M. Chen, G. Gu and L. Wu, *J. Phys. Chem.* B, **2008,** *112,* 16-22.
3. S. J. Yang and Ch. R. Park, *Nanotechnology,* **2008,** *19,* doi:10.1088/0957-4484/19/03/035609.
4. M. Li, H. Bala, X. Lv, X. Ma, F. Sun, L. Tang and Z. Wang, *Mater. Lett.,* **2007,** *61,* 690-693.
5. B. Cao and W. Cai, *J. Phys. Chem. C,* **2008,** *112*, 680-685.
6. N. Rajamanickam, S. Rajashabala and K. Ramachaudran, *J. lumin.,* **2014,** *146,* 226-233.
7. J. Zhang, J. Wang, S. Zhou, K. Duan, B. Feng, J. Weng, H. Tang and P. Wu, *J. Mater. Chem.,* **2010,** *20,* 9798-9804.
8. Y. K. Tseng, M-H. Chuang, Y. C. Chen and C. H. Wu, *J. Nanotech.* **2012,** doi:10.1155/2012/712850.
9. A. Mezni, F. Kouki, S. Romdhane, B. Warot-Fonrose, S. Joulié, A. Mlayah and L. S. Smiri, *Mater. Lett.,* **2012,** *86,* 153-156.
10. Z. Beji, T. Ben Chaabane, L. S. Smiri, S. Ammar, F. Fievet, N. Jouini and J. M. Grenèche, *Phys. Status Solidi. A*, **2006**, *203*, 504-512.
11. E. J. A. Pope and J. D. Mackenzie, *J. Non-Cryst. Solids,* **1986,** *81*, 227-237.
12. L. Poul, S. Ammar, N. Jouini, F. Fievet and F. Vilain, *J. Sol-gel Sci. Technol.*, **2003,** *26*, 261-265.
13. H. Basti, L. Ben Tahar, L. S. Smiri, F. Herbest, M.-J. Vaulay, F. Chau, S. Ammar and S. Benderbous. *J. Colloid Interface Sci.,* **2010,** *341*, 248-254.
14. S. Lee, S. Jeong, D. Kim, S. Hwang, M. Jeon and J. Moon, *Superlattices Microstruct.,* **2008,** *43* 330-339.
15. A. Dakhlaoui, M. Jendoubi, L. S. Smiri, A. Kanaev and N. Jouini, *J. Cryst. Grow.,* **2009,** *311*, 3989-3996.
16. M. Hua Wang, F. Zhou, B. Zhang and C. Yao, *J. Alloys Compd.,* **2013,** *581*, 308-312.
17. H. Basti, L. Ben Tahar, L. S. Smiri, F. Herbest, M.-J. Vaulay, F. Chau, S. Ammar and S. Benderbous. *J. Colloid Interface Sci.*, **2010,** *341*, 248-254.
18. N. R. Yogamolar and A. C. Bose, *J. Alloys Compd.*, **2011,** *509*, 8493-8500.
19. J. Xiong, U. Pal and J. G. Serrano, *J. Appl. Phys.,* **2007,** *101*, doi: 10.1063/1.2424538.
20. D. R. Lide, "CRC Handbook of Chemistry and Physics, 86 edition, CRC Press, Boca Raton, FL, USA 2005.
21. R. Viswanatha, S. Sapra, B. Satpati, P. V. Satyam, B. N. Dev and D. D. Sarma, *J. Mater. Chem.,* **2004,** *14*, 661-668.
22. A. K. Zak, R. Razali, W. H. Abd Majid and M. Darroudi, *Intern. J. Nanomedicine*, **2011,** *6,* 1399-1403.
23. N. Wang, Y. Yang and G. Yang, *Nanosc. Res. Lett.*, **2011,** *6* http: //www. nanoscalereslett. com/content/6/1/338.